Structural Eng./Earthquake Eng. Vol. 9, No. 1, 45s-55s, April 1992
Japan Society of Civil Engineers (Proc. of JSCE No. 446/I-19)

FORCED VIBRATION TESTS AND EARTHQUAKE OBSERVATION ON THE DYNAMIC RESPONSE OF RIGID EMBEDDED FOUNDATIONS

Jun'ichi TOHMA*, Keizo OHTOMO*
Teruyuki UESHIMA*
and Mikio TAKEUCHI**

This paper describes the results of basic experimental studies performed to evaluate embedment effects on the dynamic characteristics of a rigid foundation and correlation analyses between the test results and the calculated results. Field tests of a rectangular concrete block are carried out with the purpose of obtaining the basic data for verification study on analysis codes. In the correlation analyses, the methods used here are the sway-rocking model and the axisymmetric finite element model. Frequency-dependent dynamic stiffness is examined comparing those values obtained from the field tests and the elastic theories. Furthermore, the embedment effects are confirmed through earthquake observation data.

Keywords : *seismic design, soil-structure interaction, embedded foundation, earthquake observation, finite element method*

1. INTRODUCTION

In seismic design of embedded foundations, a variety of response analysis techniques have been developed to express the embedment effect of the foundation. These techniques may be roughly classified into four types ; sway-rocking (SR) model, sub-structure model, lumped mass ground (lattice) model, and finite element ground model (FEM). These techniques have been verified to give response results that are almost identical to each other under certain conditions. However, available experimental and observational data on how the vibration characteristics of the foundation change with the depth of embedment are not adequate. Verification of these analytical techniques is an important task.

An approximate analytical solution of embedded footings was developed by Beredugo and Novak[1]. Closed form formulas were proposed for frequency-dependent dynamic stiffness of cylindrical rigid footings. After that, Toki and Komatsu[2] used the elastic wave theory to analyze the dynamic stiffness for a cylindrical well foundation. They pointed out that the real part (i.e., spring effect) of the dynamic stiffness gradually decreases with the increase in frequency while the imaginary part (i.e.,radiational damping effect) increases proportionally. Kausel et al[3]. clearly defined the concept of kinematic interaction between the embedded portion of a foundation and the ground. Harada et al[4]. interpreted it as the effective input motion to the embedded portion, and indicated that the seismic response analysis with an SR model will be appropriate when the effective input motion and the dynamic stiffness are considered. After that, practical seismic response analysis methods were proposed by, for example, Yano et al[5]. and Kazama and Inatomi[6]. It was indicated that the embedment effect may be evaluated with an SR model provided adequate dynamic stiffness and effective input motions are used.

With the development of computers, more realistic seismic response analysis of a soil-structure system can be made. FEM analyses, such as FLUSH[7], are now increasingly practical. In such direct method, there are two tasks.

① Effects of that the foundation is 3-dimensional.

② Wave dissipation at the soil model boundaries.

If their treatments are appropriate in modelling, the embedment effect will be faithfully reflected in the model. Moreover, as the stress and strain of each element of the ground can be determined, it has a merit that the ground stability can be evaluated in detail.

As discussed above, at present, various analytical models can express the embedment effect. It is essential to clarify the dynamic characteristics of the foundation on the actual ground, compare them with the analytical results, and accumulate such verification data[8),9)].

This paper reports the results of a verification of embedment effect through forced vibration tests and earthquake observation. A rigid rectangular foundation (a concrete block) was placed on a soft ground, and its depth of embedment was set at various levels. Dynamic stiffness of the ground,

* M. of JSCE, M. Eng., Central Research Institute of Electric Power Industry (1646, Abiko, Abiko-shi, Chiba 270-11)
** M. of JSCE, M. Eng., Okumura Corporation

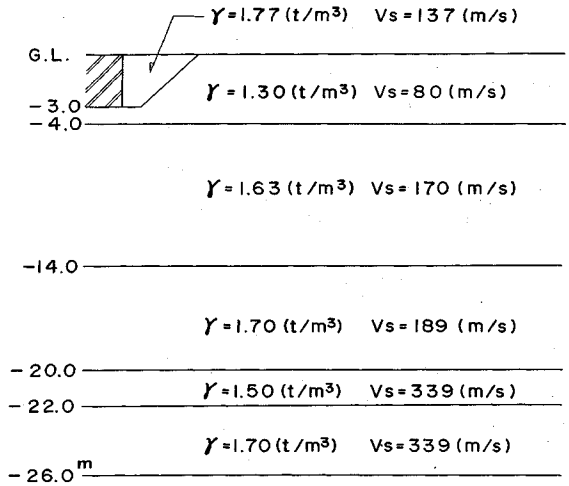

Fig.1 Soil layers at the site.

Table 1 Excitation test cases

	height (m)	embedment (m)	cross section
case 1	1.5	0	
case 2	3.0	0	
case 3	3.0	1.5	
case 4	3.0	3.0	

which are required in the SR model, were examined on the basis of experimental results. Moreover, numerical simulation with an FEM model was made to verify the appropriateness of the axisymmetric modelling for a rectangular foundation. The characteristics of dynamic behaviors depending on the presence or absence of embedment were also identified from the results of earthquake observation.

2. GROUND CONDITIONS

The ground comprises, from the surface to a depth of 4 m, a soft Kanto loam layer of which *N*-value is about 4. Beyond that, silt layers and sand layers form alternate strata. The bottom of the foundation is placed on the loam layer at G.L. − 3.0 m. Silty sand was used to back-fill the foundation. The structure of the ground layers is shown in **Fig.1**.

3. METHODS OF EXPERIMENTS AND OBSERVATION

Forced vibration tests and earthquake observation were made for four cases shown in **Table 1**. The four cases are various combinations of the foundation height and the depth of embedment.

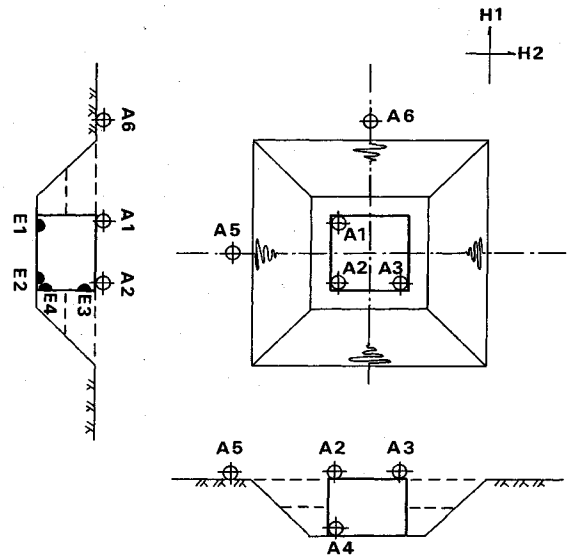

Fig.2 Representative measuring points.

The forced vibration tests were made with a shaker whose maximum exciting force was 10 tf. Shakings in two horizontal perpendicular directions (denoted as H1 and H2) and a shaking in vertical direction were made separately with the shaker placed on the top of the foundation. The standard layout of measuring points is shown in **Fig.2**. The eccentric mass moment of the shaker was kept constant during the shaking, and the frequency was varied stepwise. To examine possible effects of the soil non-linearity and the degree of disturbance within soils, tests were also made by changing the eccentric mass moment. The results of experiments, however, had reproducibility, and such effects were not observed. The responses were considered to be within the elastic range.

In this paper, we discuss the horizontal H2 shaking which were performed with the constant eccentric mass moment of 0.968 kgm and with the frequency range up to 20 Hz. Micro tremor and earthquake observation were made for this soil-foundation using the same measuring system.

4. Results of Forced Vibration Tests

(1) Basic Dynamic Characteristics of the Model Foundation

The case 2 (foundation height of 3.0 m, without embedment) will be taken as a basic case. The response characteristics of the case during a

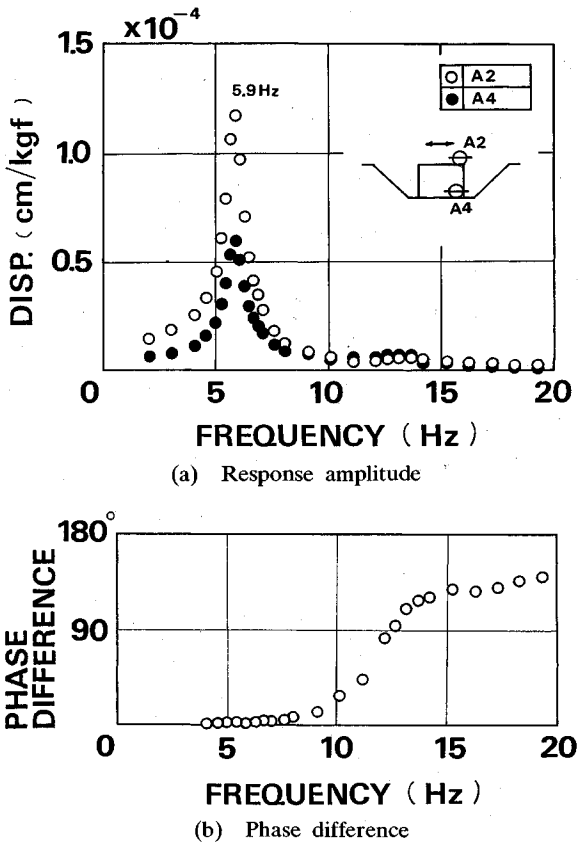

(a) Response amplitude

(b) Phase difference

Fig.3 Frequency response of the non-embedded foundation.

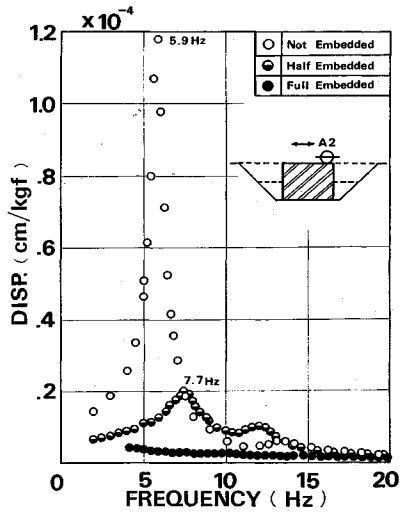

Fig.4 Comparison of the frequency responses due to embedment under horizontal excitation.

horizontal shaking (H2) will be examined.

Fig.3 (a) compares the horizontal response amplitudes of two measuring points. One point (A2) is on the top of the foundation, and the other (A4) near the bottom of the foundation. The response amplitude is expressed as the half amplitude of displacement (cm/kgf) for unit shaking force. **Fig.3** (b) shows the phase difference between the two measuring points. These diagrams indicate that, up to a little over the first resonant frequency (5.9 Hz), the response amplitude on the foundation top is larger than that near the bottom, and there is almost no phase difference between the two measuring points. Thus the first mode of sway-rocking (i.e., lower center rocking) is predominant. At higher frequencies, however, there are phase differences between the two measuring points, and the response amplitude near the foundation bottom exceeds that on the top although the difference is small. Thus the second mode of sway-rocking (i.e., upper center rocking) is present.

(2) Dynamic Characteristics of the Foundation at Different Depths of Embedment

To examine the dynamic characteristics of the foundation at various depths of embedment, the resonance curves were compared with each other.

The resonance curves of the horizontal response at the foundation top (A2) under horizontal excitation are shown in **Fig.4**. The deeper is the embedment, the smaller is the response amplitude. Thus the damping effect of the ground tends to increase with the depth of embedment. The peak frequency of the resonance curve of the non-embedded case is 5.9 Hz, and that of the half-embedded case is 7.7 Hz. Obviously these are the soil-structure interaction (SSI) system frequencies. Thus the rigidity of the ground shows a tendency to increase with the presence of embedment. In the case of full-embedment, the response amplitude is very small, and its peak is not certain.

(3) Horizontal Motion and Rotational Motion of the Foundation at Its Center of Gravity

The vibration of the foundation may be considered as a rigid body motion, and can be treated as a coupled horizontal and rocking vibration system. Accordingly, the horizontal amplitude and the angle of rotation at the center of gravity of the foundation can be computed from the horizontal motions and vertical motions at two measuring points (A2 and A3) on the top of the foundation.

a) Without Embedment

Fig.5 shows that the first SSI system frequency is 5.9 Hz. The second SSI system frequency is 13.2 Hz.

b) Half-Embedment

Fig.6 shows that the first SSI system frequency is 7.7 Hz. The second SSI system frequency is 12.0 Hz. One special characteristic is that the angle of

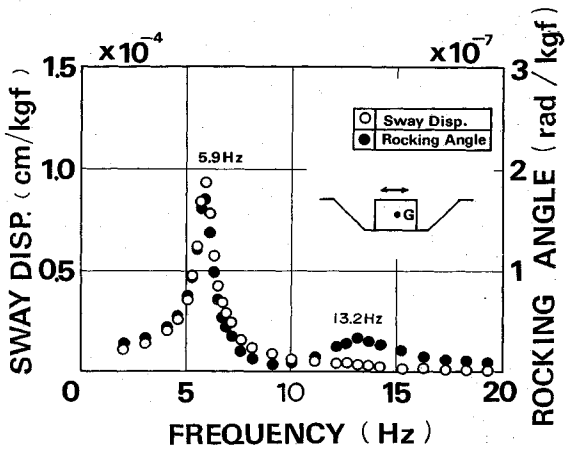

Fig.5 Swaying and rocking responses of the non-embedded foundation.

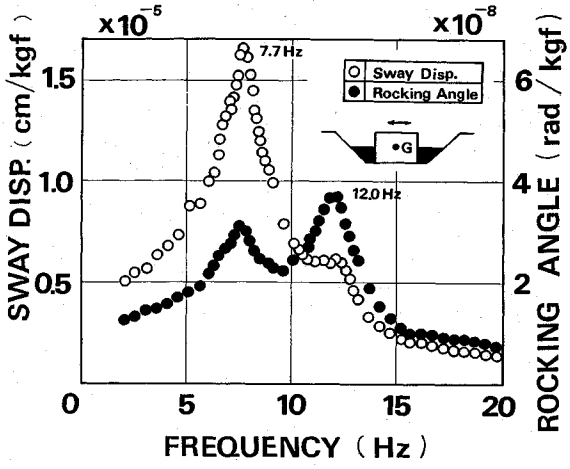

Fig.6 Swaying and rocking responses of the half-embedded foundation.

rotation of the second mode is greater than that of the first mode.

c) Full-Embedment

Fig.7 shows no clear peak in the horizontal motion, and the amplitude decreases with the increase in frequency. On the other hand, there is a peak at 9.9 Hz in the rotational motion.

(4) Evaluation of Dynamic Stiffness of Foundation Base Ground

We evaluated the dynamic stiffness of the base and lateral ground separately. First, it is necessary to examine the dynamic stiffness of the ground beneath the bottom of the foundation without embedment. According to the methodology of Hirata et al.[10], the frequency dependency of the dynamic stiffness were determined from the results of the forced vibration tests. An ordinary SR model was assumed as shown in **Fig.8**. The horizontal

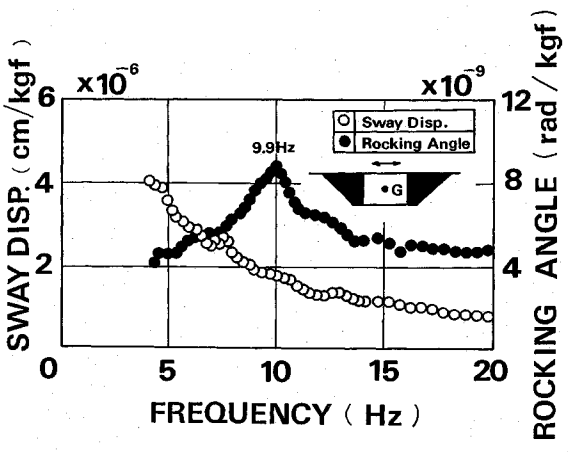

Fig.7 Swaying and rocking responses of the full-embedded foundation.

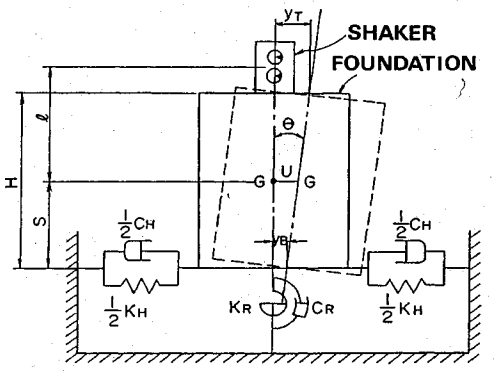

Fig.8 A sway-rocking model for the non-embedded foundation.

displacement and angle of rotation of the center of gravity shown in **Fig.5** were given to the following equation of motion of the model by frequency to determine the dynamic stiffness of the base ground.

$$[M]\{\ddot{X}\}+[C]\{\dot{X}\}+[K]\{X\}=\{F\} \quad \cdots\cdots(1)$$

Where

$$\{X\}=\begin{Bmatrix} u \\ \theta \end{Bmatrix} \quad \cdots\cdots(2)$$

$$\{F\}=m_0 r\omega^2 e^{i\omega t}\begin{Bmatrix} 1 \\ l \end{Bmatrix} \quad \cdots\cdots(3)$$

$$[M]=\begin{bmatrix} M & 0 \\ 0 & I_G \end{bmatrix} \quad \cdots\cdots(4)$$

$$[C]=\begin{bmatrix} C_H & -C_H S \\ -C_H S & C_R+C_H S^2 \end{bmatrix} \quad \cdots\cdots(5)$$

$$[K]=\begin{bmatrix} K_H & -K_H S \\ -K_H S & K_R+K_H S^2 \end{bmatrix} \quad \cdots\cdots(6)$$

Where u : Horizontal displacement of the center of

gravity of the foundation ; θ : Angle of rotation of the foundation ; M : Total mass of the foundation and the shaker ; I_G : Moment of inertia of the mass around the center of gravity ; C_H : Horizontal damping coefficient of the base ground ; C_R : Rotational damping coefficient of the base ground ; K_H : Horizontal spring coefficient of the base ground ; K_R : Rotational spring coefficient of the base ground ; S : Distance between the center of gravity of the foundation-shaker system and the point of action of the soil spring ; l : Distance between the center of gravity of the foundation-shaker system and the point of action of the shaking force ; $m_0 r$: Eccentric mass moment of the shaker ; ω : Circular excitation frequency ; and i : the imaginary unit ($=\sqrt{-1}$).

The horizontal displacement u and the angle of rotation θ of the center of gravity of the foundation can be expressed by the following equations, respectively.

$$\left.\begin{aligned} u&=Ue^{iwt}\\ \theta&=\Theta e^{iwt}\end{aligned}\right\} \cdots\cdots(7)$$

Where U and Θ are their respective amplitudes given in complex numbers. K_H is the dynamic stiffness in the horizontal direction, and K_R is the dynamic stiffness in the rotational direction. These coefficients are shown in the following equations.

$$\left.\begin{aligned} K_H&=K_H+iK_H'\\ K_R&=K_R+iK_R'\end{aligned}\right\} \cdots\cdots(8)$$

Where,

$$\left.\begin{aligned} K_H'&=\omega C_H\\ K_R'&=\omega C_R\end{aligned}\right\} \cdots\cdots(9)$$

When Eqs.(7) and (8) are substituted in Eq.(1), the dynamic stiffness in the horizontal direction is determined by the following equation.

$$K_H=\frac{m_0 r\omega^2+M\omega U}{U-S\Theta} \cdots\cdots(10)$$

K_H values obtained from Eq.(10) are shown in **Fig.9**. The dynamic stiffness of the rotational direction is similarly given by the following equation.

$$K_R=\frac{(l+S)m_0 r\omega^2+\omega^2(SMU+I_G\Theta)}{\Theta} \cdots\cdots(11)$$

K_R values obtained from Eq.(11) are shown in **Fig.10**.

In **Figs.9** and **10**, the theoretical solutions given by the elastic half space theory of Tajimi[11] are indicated by Solid lines. In obtaining these values, the contact pressure distribution of the foundation was assumed to be uniform. (Triangular distribution was assumed for rotation.) The shear wave velocity (V_s) applied to the theoretical solutions was selected in such a way that the experimental value of the real part of the dynamic stiffness at the first SSI system frequency of the foundation could be reproduced.

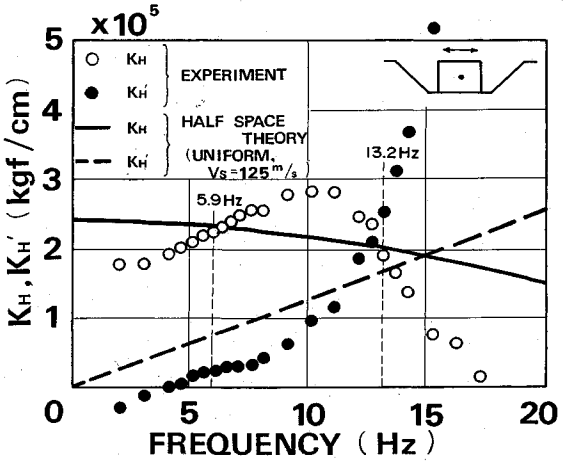

Fig.9 Horizontal dynamic stiffness of the base ground.

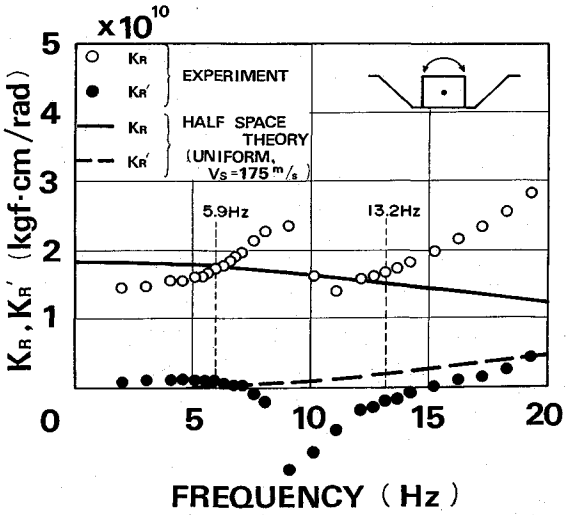

Fig.10 Rotational dynamic stiffness of the base ground.

Within a range up to the first SSI system frequency (5.9 Hz) of the foundation, the dynamic stiffness obtained by experiments agreed relatively well with theoretical solutions in both the real and imaginary parts for both the horizontal and rotational movements. In the frequency range exceeding the first SSI system frequency, the experimental values showed complicated variations. They are characterized in that from the second SSI system frequency (13.2 Hz) and beyond, K_H decreases and K_R increases.

The shear wave velocities used in the abovementioned work are shown in **Table 2**. The table also shows the values of the equivalent shear wave

Table 2 Comparison of equivalent shear wave velocities ; Vs (m/s).

	by the excitation tests		by the elastic
	case 1	case 2	layered model
horizontal	115	125	134
rotational	165	175	159

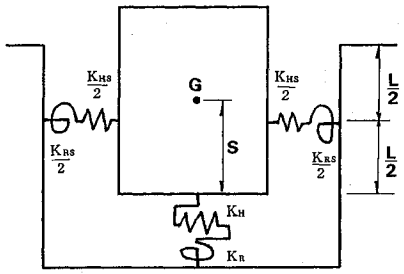

Fig.11 A sway-rocking model for the embedded foundation.

velocities(V_s), which are determined from the ground layer model by giving the stratification correction according to Tajimi's method[11]. The equivalent V_s for the rotational motion is greater than that for the horizontal motion, indicating the effects of the stratification. As for the V_s values obtained from the forced vibration tests, the V_s value of the case 2 (the foundation height : 3 m ; the contact pressure: 6.9 tf/m^2) is greater than that of the case 1 (the foundation height : 1.5 m ; the contact pressure : 3.45 tf/m^2), indicating that the V_s value changed with the contact pressure. In other words, the values of V_s obtained in the experiment showed a dependency on restraint. The values of the equivalent V_s based on the ground layer model do not reflect any consideration of the dependency on restraint.

As discussed above, the magnitude of the dynamic stiffness of the base ground of a foundation without embedment can be explained mostly by the elastic half space theory when the soil layering is considered. At higher frequencies exceeding the first SSI system frequency, however, the theoretical values and the experimental values showed some discrepancies. This point needs investigation in future.

(5) Evaluation of Dynamic Stiffness of the Lateral Ground of the Foundation

To evaluate the dynamic stiffness of the ground on the sides of the foundation, an SR model which considers embedment was set as shown in **Fig.11**. The experimental values of the horizontal displacement and the angle of rotation of the center of gravity were given to the following equation of motion for the model by frequency, and the dynamic stiffness of the lateral ground were obtained.

$$[M]\{\ddot{X}\}+[C']\{\dot{X}\}+[K']\{X\}=\{F\} \quad \cdots\cdots (12)$$

Where,

$$[C']=\begin{bmatrix} C_H+C_{HS} & -C_HS-C_{HS}\left(S-\frac{L}{2}\right) & -C_HS-C_{HS}\left(S-\frac{L}{2}\right) \\ -C_HS-C_{HS}\left(S-\frac{L}{2}\right) & C_R+C_{RS}+C_HS^2+C_{HS}\left(\frac{L^2}{3}-LS+S^2\right) & \end{bmatrix} \quad \cdots\cdots (13)$$

$$[K']=\begin{bmatrix} K_H+K_{HS} & -K_HS-K_{HS}\left(S-\frac{L}{2}\right) & -K_HS-K_{HS}\left(S-\frac{L}{2}\right) \\ -K_HS-K_{HS}\left(S-\frac{L}{2}\right) & K_R+K_{RS}+K_HS^2+K_{HS}\left(\frac{L^2}{3}-LS+S^2\right) & \end{bmatrix} \quad \cdots\cdots (14)$$

Where, K_{HS} : Horizontal spring coefficient of the lateral ground ; C_{HS} : Horizontal damping coefficient of the lateral ground ; K_{RS} : Rotational spring coefficient of the lateral ground ; C_{RS} : Rotational damping coefficient of the lateral ground ; L : Depth of embedment.

The following dynamic stiffness of the lateral ground were calculated in a manner similar to that used for the base ground.

$$\left.\begin{aligned} \boldsymbol{K}_{HS}&=K_{HS}+iK'_{HS} \\ \boldsymbol{K}_{RS}&=K_{RS}+iK'_{RS} \end{aligned}\right\} \quad \cdots\cdots (15)$$

Where,

$$\left.\begin{aligned} K'_{HS}&=\omega C_{HS} \\ K'_{RS}&=\omega C_{RS} \end{aligned}\right\} \quad \cdots\cdots (16)$$

In Eq.(12), it is necessary to know the frequency-dependency of the dynamic stiffness of the base ground in advance. The results of the forced vibration tests on the foundation without embedment (**Figs.9 and 10**) were used here.

For the cases of half-embedment and full-embedment, the real parts (K_{HS}) of the horizontal dynamic stiffness of the lateral ground are shown for the frequency range from 0 to 10 Hz in **Fig.12**. The imaginary parts (K'_{HS}) are also comparatively shown in **Fig.13**. With the embedment, the imaginary part of the dynamic stiffness increases in proportion with the increase in frequency ; the effect of radiational damping is conspicuous. This point agrees with the results of the study for cylindrical well foundations by Toki and Komatsu[2].

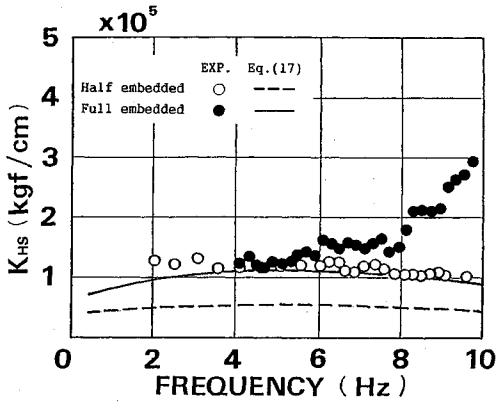

Fig.12 Comparison of the real part of horizontal dynamic stiffness ; K_{HS}.

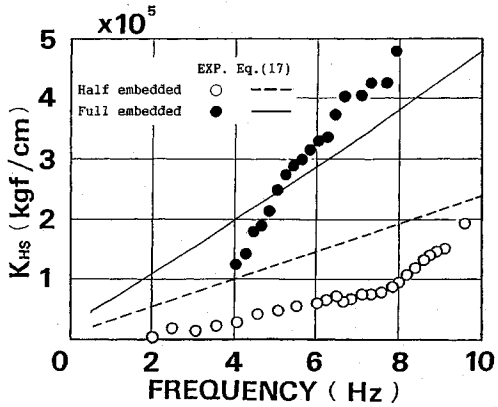

Fig.13 Comparison of the imaginary part of horizontal dynamic stiffness ; K'_{HS}.

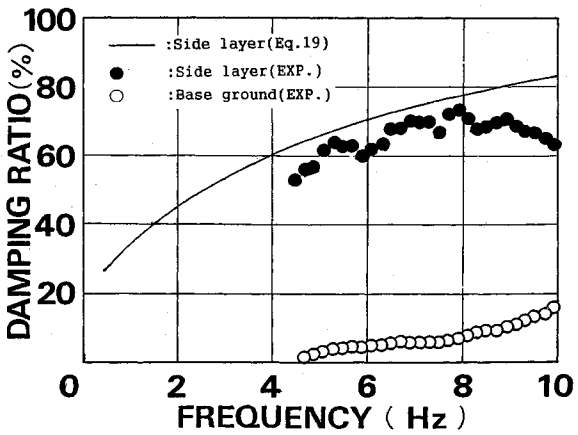

Fig.14 Equivalent damping ratio of the ground.

For a case where a cylindrical rigid body foundation buried in an elastic ground is subjected to horizontal displacement, the theoretical solutions of the dynamic stiffness of the lateral ground are given by Beredugo and Novak[3] as follows :

$$\left.\begin{aligned} K_{HS} &= L\cdot Gs\cdot S_{u1} \\ K'_{HS} &= L\cdot Gs\cdot S_{u2} \end{aligned}\right\} \quad \cdots\cdots(17)$$

Where L : Depth of embedment ; G_s : Shear modulus of the lateral ground ($=\rho V_s^2$) ; V_s : Shear wave velocity of the lateral ground ; ρ : Density of the lateral ground ; S_{u1} : Nondimensional parameter indicating frequency-dependency of K_{HS} ; S_{u2} : Nondimensional parameter indicating frequency-dependency of K'_{HS}.

The values of S_{u1} and S_{u2} are obtained as the real part and the imaginary part of a complex function expressed by the following equation :

$$S_u(a_0,\nu)=G_s[S_{u1}(a_0,\nu)+iS_{u2}(a_0,\nu)]=2\pi G_s a_0 \frac{\frac{1}{\sqrt{q}}H_2^{(2)}(a_0)H_1^{(2)}(\chi_0)+H_2^{(2)}(\chi_0)H_1^{(2)}(a_0)}{H_0^{(2)}(a_0)H_2^{(2)}(\chi_0)+H_0^{(2)}(\chi_0)H_2^{(2)}(a_0)} \quad \cdots\cdots(18)$$

where $q=(1-2\nu)/2(1-\nu)$; ν : Poisson's ratio ; $\chi_0 = a_0\sqrt{q}$; a_0 : Nondimensional frequency ($= r_0\omega/V_s$) ; r_0 : Equivalent radius of the foundation ; and $H_n^{(2)}$: Hankel function of the second kind of order n.

In order to apply Eq.(18) to the rectangular model, the equivalent radius of the model was set so that the bottom area equals circular area with radius r_0.

The theoretical solutions obtained from Eq.(18) by setting $V_s=80$ m/s and $\nu=0.4$ are shown in **Figs.12** and **13**. When compared with experimental values, the solutions based on the elastic theory are able to explain mostly the dynamic stiffness of the lateral ground of the embedment.

Next, the equivalent viscous damping constant(h_{HS}) of the lateral ground in its horizontal direction can be obtained by the following equation[12].

$$\frac{h_{HS}}{1-h_{HS}^2}=\frac{K'_{HS}}{2K_{HS}} \quad \cdots\cdots(19)$$

The frequency-dependency of h_{HS} is shown in **Fig.14**. The equivalent viscous damping constant derived from Eq.(19), by its definition, does not depend on the depth of embedment. It is a function of the nondimensional frequency number and Poisson's ratio. In the diagram, the results of the forced excitation tests and the results obtained from Eq.(19) are compared with each other. **Fig.14** shows that the equivalent viscous damping of lateral ground of embedded rectangular foundations can be mostly estimated by Eq.(19). The experimental equivalent viscous damping for base ground is comparatively shown in **Fig.14**. It is obvious that the radiation damping to the lateral ground is greater than to the base ground.

From the discussion above, it can be concluded

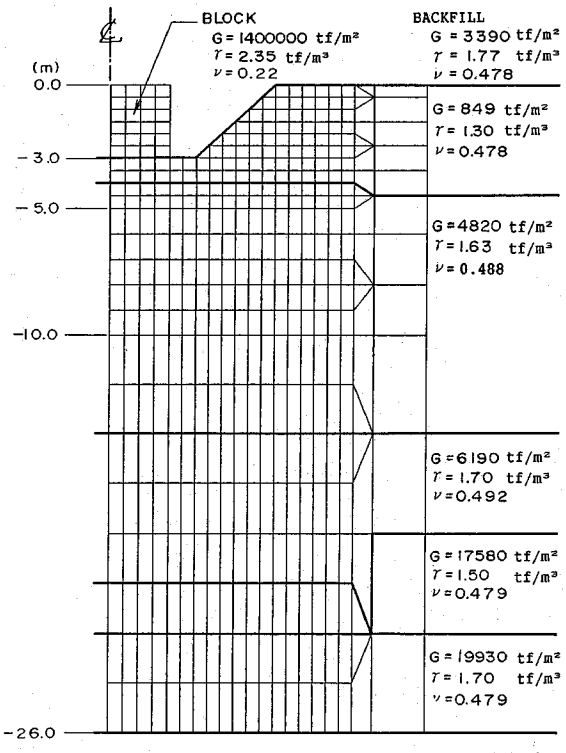

Fig.15 An axisymmetric finite element model for simulation of the excitation tests.

as follows: When an embedded rectangular foundation is expressed by an SR model, the dynamic stiffness may be estimated approximately from the solutions of the elastic theory derived for a cylindrical rigid body considering the equivalent radius.

5. SIMULATION OF FORCED VIBRATION TESTS WITH AN AXISYMMETRIC FEM

A program for 3-dimensional seismic response analysis by complex stiffness, TB3D, was used to simulate the behavior of the foundation under external shaking. The program was developed by Ueshima et al[13]. In the analysis, to consider the 3-dimensional effects of a rectangular foundation, an axisymmetric model, which is symmetric with respect to the vertical axis passing through the center of the foundation, was used. **Fig.15** shows the diagram of division of the soil-structure system into elements. In this case, the equivalent radius of the rectangular foundation was set so that the bottom area of the FEM model equals the bottom area of the experimental model foundation. The ground model was provided with a transmitting boundary on its side, and a viscous boundary on the bottom, to take wave dissipation into consideration.

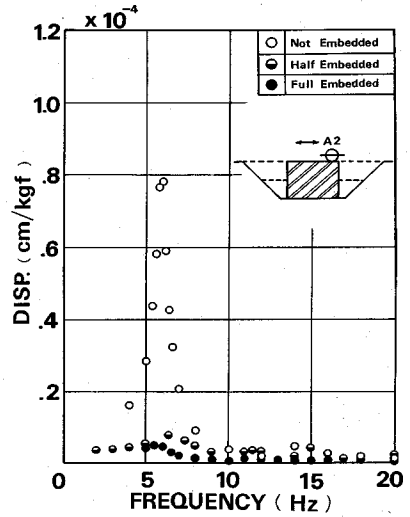

Fig.16 Simulated frequency responses from the FEM analyses.

Steady-state responses of the system when a unit exciting force is applied to the top of the foundation were determined. The frequency was varied stepwise. **Fig.16** shows the results of simulations of forced vibration tests on the foundation without any embedment, with half embedment, and with full embedment, respectively. Comparison of such results with those of the experiment (**Fig.4**) indicates that the decrease in amplitude with the embedment is expressed relatively well.

6. CONFIRMATION OF THE EMBEDMENT EFFECT THROUGH EARTHQUAKE OBSERVATION

(1) Comparison of Maximum Response Values

The correlation between the maximum ground surface velocity and the maximum velocity on the foundation top was examined for the respective groups of the two cases ; without embedment and with full embedment. The standard measuring point (SP) of the ground surface is about 30 m away from the foundation and is considered to be free of any effects of the presence of the foundation.

Fig.17 (a) shows the results of the case without embedment. The responses on the top(A2) of the foundation exceed those on the ground surface. **Fig.17** (b) shows the results of the case with full embedment. In this case, the responses on the ground surface are smaller than or almost comparable to the responses on the foundation top. In other words, when embedded, the foundation does not make responses predominant over these of the surrounding ground.

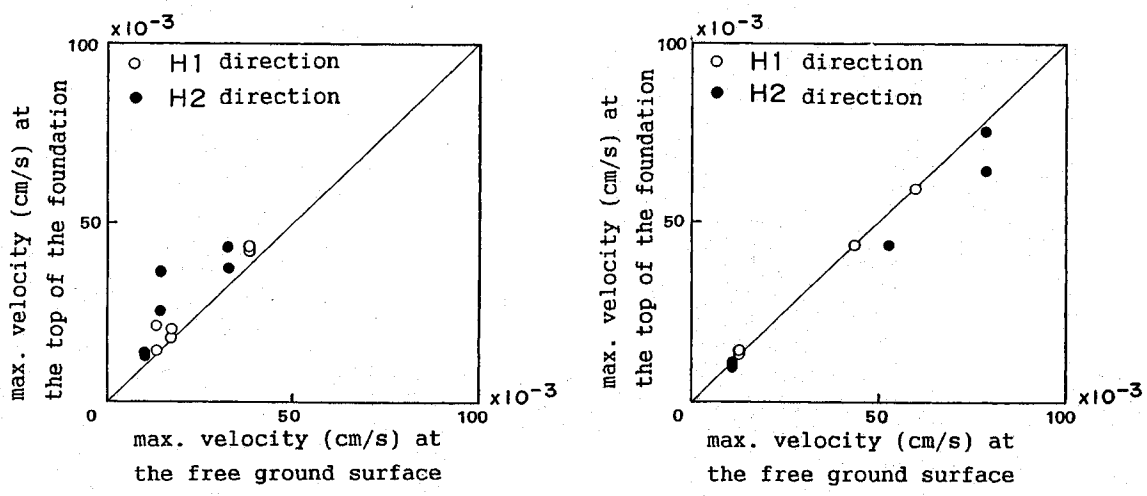

(a) the non-embedded foundation (b) the full embedded foundation

Fig.17 Comparison of the maximum velocities of the ground and the foundation subjected to earthquake motions.

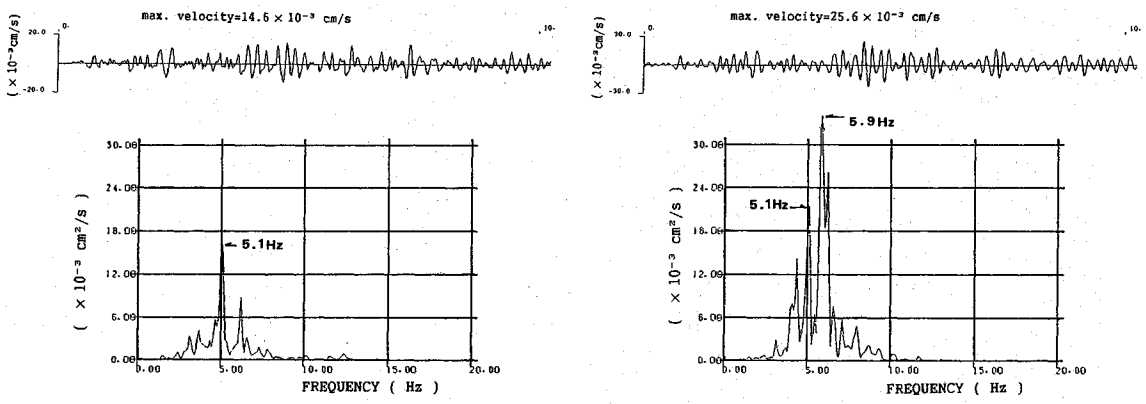

(a) free ground surface (SP) (b) foundation surface (A2)

Fig.18 An example of the earthquake response of the non-embedded foundation.

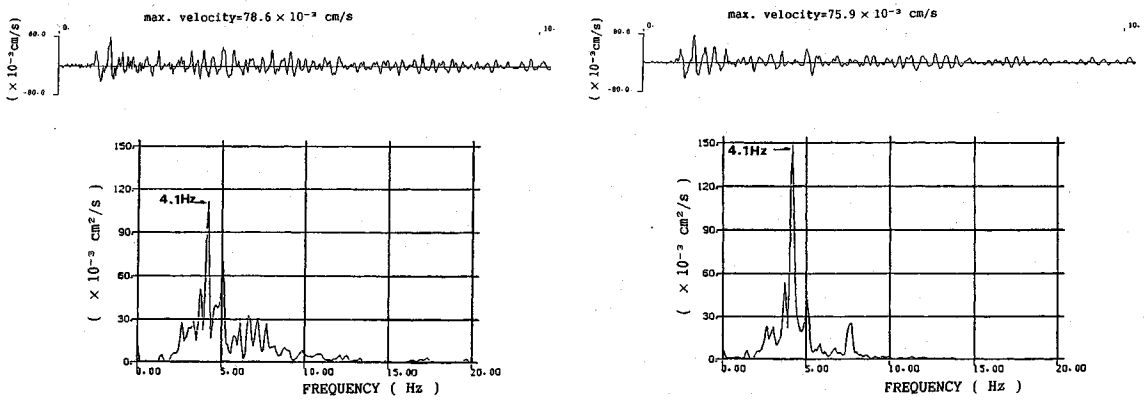

(a) free ground surface (SP) (b) foundation surface (A2)

Fig.19 An example of the earthquake response of the full-embedded foundation.

(2) Frequency Response Characteristics of the Foundation

How the embedment changes the frequency response characteristics of the foundation is shown for the following two cases.

a) Without any embedment

Fig.18 compares the power spectra taken on the foundation (A2) and on the ground surface(SP) simultaneously. On the ground surface, there is a peak at 5.1 Hz. On the foundation, there is a similar peak at 5.1 Hz, but the most predominant peak is at 5.9 Hz. Since the peak of the response of the foundation during the forced vibration test was at 5.9 Hz, it may be thought that the motion was amplificated at the first SSI system frequency by the seismic motion. Any components which appear in both spectra on the ground and on the foundation, such as the peak at 5.1 Hz are considered to be the predominant components of the ground or earthquake motion itself.

b) With full embedment

In this case, as shown in **Fig.19**, there are no large values except a peak of 4.1 Hz which is common to both the ground surface and the foundation. Thus the vibration characteristics of the foundation are mostly identical to those of the ground surface. Any SSI system frequencies are not identified.

(3) Earthquake Motion Loss Mechanism of Embedded Foundation

Fig.20 shows the Fourier spectrum ratio (i.e., a transfer function) of the horizontal motion on the full-embedded foundation top (A2) normalized by the corresponding ground surface motion (SP) based on the recorded motions shown in **Fig.19**. The transfer function thus obtained has many spikes. If such spikes are neglected, the overall trend can be seen. The ratio is around 1.0 from 0 to 5 Hz, and the ratio drops gradually in accordance with the frequency increase. The amplitude of the foundation response is smaller than that of the ground at higher frequencies. It may be attributed to the foundation's loss mechanism of earthquake motion[14] ; since the rigidity of the foundation is greater than that of the ground, the foundation suppresses shorter seismic wave lengths.

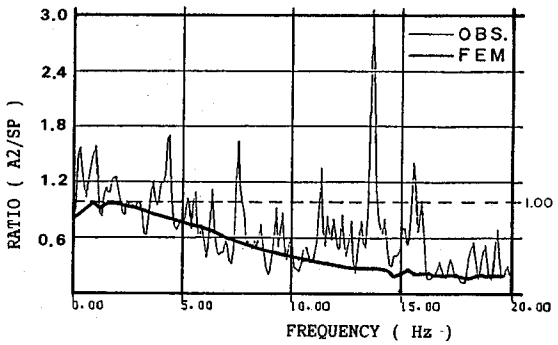

Fig.20 Transfer function of the earthquake motion between the full-embedded foundation and the ground surface.

7. CONCLUSIONS

The embedment effect was examined through the forced vibration tests and earthquake observation on a rectangular rigid foundation placed on a soft ground within the elastic range. Findings were as follows :

(1) When subjected to horizontal shaking, the foundation exhibited sway and rocking as a rigid body. In the case of no embedment, the lower center rocking, which is the first SSI system frequency, was predominant during the forced vibration tests as well as earthquake observation.

(2) When subjected to horizontal shaking, the embedded foundation also exhibited sway and rocking. The SSI system frequency was high and the amplitude was smaller in comparison with the foundation without embedment.

(3) The frequency-dependency of the dynamic stiffness of the base ground were successfully approximated with semi-infinite elastic solutions using equivalent shear wave velocities. However, in a higher frequency range where the upper center rocking was observed, the difference between the experimental value and the theoretical value was large.

(4) When the dynamic stiffness of the ground on the side of the embedment were determined by forced vibration tests, the value of the imaginary part was found to be increased significantly by embedment. In other words, the effect of radiational damping was greater. The tendency was generally explainable with the elastic theory for a cylindrical foundation.

(5) The forced vibration tests were simulated by an axisymmetric FEM analysis. The decrease in the resonance amplitude of the foundation due to the embedment was represented relatively well. The axisymmetric modelling was found to be effective for expressing the embedment effect of the rectangular foundation.

(6) The earthquake observation showed that the response of the embedded foundation was smaller than the response on the ground surface at higher frequencies. It may be attributed to the foundation's loss mechanism of earthquake motion.

REFERENCES

1) Beredugo, Y.O. and Novak,M. : Coupled horizontal and

rocking vibration of embedded footing, Canadian Geotechnical Journal, Vol.9, No.4, pp.477～497, 1972.

2) Toki, K. and Komatsu, A. : Seismic response of well foundation, Proc. of JSCE, No.281, pp.29～40, 1979 (in Japanese).

3) Kausel, E. et al. : Dynamic analysis of embedded structures, Trans. of 4th SMiRT, K2/6, pp.1～10, 1977.

4) Harada, T. et al. : Dynamic soil-structure interaction analysis by continuum formulation method, Report of the Institute of Industrial Science, the Univ. of Tokyo, Vol.29, No.5, 1981.

5) Yano,A. et al. : Earthquake response analysis method for embedded reactor buildings (Part 1～4),Proc.of Annual Conference of AIJ, pp.199～206, 1987 (in Japanese).

6) Kazama, M. and Inatomi, T. : Earthquake response analysis for embedded rigid structures using a rigid body-ground spring model, Proc. of JSCE, No.410/I-12, pp.138～147, 1989 (in Japanese).

7) Lysmer, J. et al. : 'FLUSH'-A computer program for approximate 3-D analysis of soil-structure interaction problems, Report No. EERC 75-30, Univ. of California, Berkeley, 1975.

8) Fujimori, T. et al. : Large-scale model forced-vibration test on wave radiation characteristics of surrounding ground and evaluation of radiation damping, Proc. of the 8th JEES, pp.1011～1016, 1990 (in Japanese).

9) Fukuoka, A. et al. : Experimental study on embedded structure-soil interaction, Proc. of the 8th JEES, pp.1029～1034, 1990 (in Japanese).

10) Hirata, K. et al. : Evaluation of elastic and damping characteristics of bedrock by the vibration test of the foundation (Part 1 and Part 2), Proc. of the 6th JEES, pp.1673～1688, 1982 (in Japanese).

11) Tajimi, H. et al. : Earthquake Engineering, pp.53～100, Shokokusha Co., Ltd., 1977 (in Japanese).

12) Tajimi, H. : Introduction to Structural Dynamics, pp.27～31, Corona Publishing Co., Ltd., 1984 (in Japanese).

13) Ueshima, T. et al. : Development of a computer program for 3-D complex response analysis of soil-structure interaction problems with transmitting boundaries, Report of Central Research Institute of Electric Power Industry, No.382009, 1982 (in Japanese).

14) Sawada, Y. et al. : Loss mechanism of earthquake motion on foundation, Proc. of the 6th JEES, pp.1553～1560, 1982 (in Japanese).

(Received May 20, 1991)

埋込みのある剛体基礎の動的応答に関する起振実験と地震観測

当麻純一・大友敬三・上島照幸・竹内幹雄

本論文は，正方形の底面形状を有する剛体基礎の埋込み効果を評価することを目的としている．まず，原位置でコンクリートブロックの起振実験を行い，スウェイ・ロッキングモデルに必要な地盤の動的抵抗係数を求め，弾性理論解と比較検討した．つぎに，有限要素法によるシミュレーション解析結果を起振時応答結果と照合し，軸対称モデル化の妥当性を検討した．最後に，基礎の地震観測により埋込み効果を確証した．